Modulation and Coding Optimization for Energy Harvesting Transmitters

Qing Bai and Josef A. Nossek
Institute for Circuit Theory and Signal Processing
Technische Universität München, Munich, Germany
Email: bai.qing@nws.ei.tum.de

***Abstract*—Energy harvesting communication devices, which are able to convert different forms of ambient energy to electrical energy and use it for communications, have emerged as an alternative to the conventional devices powered by fixed utilities or batteries, due to their potential to be deployed in less accessible environments and to operate for longer time without any human intervention. As the energy input to such systems is in general non-constant, new resource management principles and resource allocation algorithms need to be developed. In this work, we evaluate the performance limit of energy harvesting transmitters in terms of throughput when only discrete modulation levels and coding rates are applicable, assuming perfect knowledge of energy arrivals and constant channel state during the time slot of interest. In addition, we employ a detailed circuit power model to account for the energy consumption within the transmitter circuitry. A throughput-maximizing energy expenditure trajectory can be obtained with the construction algorithm we propose which utilizes the Pareto boundary of the system on the power-rate graph, and it corresponds to an optimal adaptive modulation and coding strategy that the transmitter should employ.**

I. Introduction

With the development of energy harvesting technology, communication devices with energy harvesting ability have become feasible, which motivates a lot of research activities recently concerning their utilization in point-to-point communications or in networks, *e.g.*, [1][2][3]. These devices find especially important applications in wireless sensor networks due to the extended lifetime they can offer. However, for the typical communication range in a wireless sensor network which is rather short, the transmit power required to achieve a sufficiently good receive signal-to-noise ratio (SNR) is not significantly larger than the analog/digital processing power of the transmitting node [4][5]. This means, to evaluate the performance of a short-range communication system with energy harvesting nodes, an accurate energy consumption model of the nodes, which includes not only radiated energy but also circuit energy consumption, has to be considered. Apart from that, new design challenges are posed in the pursuit of efficient energy usage of an energy harvesting node, as the energy sources are usually not controllable and the energy that becomes available at the node can be unsteady and even unpredictable. All these considerations call for the establishment of a suitable optimization framework for energy harvesting nodes, within which effective energy allocation algorithms with low complexity can be developed.

We focus on an energy harvesting transmitter which aims at maximizing its throughput over a limited time slot, and try to find the optimal mode of operation (MOP) it should employ which changes over time depending on the energy arrivals and the energy storage capacity of the node. This optimization framework was proposed in [6][7]. We integrate the important circuit power model into the framework and study its effect on the optimal MOP. We have followed the information theoretic approach in our previous works [8][9] and employed a continuous power model for the transmitter. Now we consider discrete MQAM modulations and coding rates instead, and it turns out that once we determine the *energy-efficient* MOPs of the system, the optimization algorithm we developed in [8][9] can be modified in a straightforward fashion to produce the optimal or a near-optimal solution in the new scenario.

The rest of the paper is organized as follows: in Section II, the system model is introduced from the aspects of wireless channel, circuit power, uncoded/coded data transmission, and energy harvesting and expenditure. The throughput maximization problem is formally given in the end. In Section III, we first review the optimal transmission strategy with the continuous power model and the critical slope based optimization algorithm. Then we define and determine the energy-efficient MOPs for both uncoded and coded transmissions, which are crucial in the application and modification of the existing algorithm. The construction procedure of an optimal or near-optimal energy expenditure trajectory is described in Section IV, where several *smoothing* schemes are also discussed. Simulation results are shown in Section V before we draw conclusions in Section VI.

II. System Model and Problem Formulation

We investigate the exploitation of energy during the time slot $[0, T]$ by an energy harvesting transmitter, which has enough data to deliver to a receiver d meters apart. The notations and values of the system parameters are summarized in Table I, where f_{c} represents the carrier frequency and B stands for the bandwidth used for transmission. The symbol duration T_{s} is approximated by $1/B$. Other parameters in Table I will be explained later in this section.

A. Channel Model

The wireless channel between the transmitter and the receiver is assumed invariant during $[0, T]$ and we consider only the path loss for the radio propagation effect. Let p_{tx} be the

ISBN 978-3-8007-3482-5

transmit power and p_{rx} be the corresponding receive power. Assuming that the distance d between the transmitter and the receiver is also constant in $[\,0, T\,]$, we write the signal-to-noise ratio (SNR) at the receiver as [4][10]

$$\gamma = \frac{p_{\mathrm{rx}}}{N_0 B} = \frac{p_{\mathrm{tx}}}{M_{\mathrm{l}} G_1 d^{\kappa} N_0 B},$$

where $\frac{N_0}{2}$ is the noise power spectrum density, κ is the path loss exponent, and G_1 is the the power gain factor at the reference distance of 1 meter which is dependent on the antenna patterns and the wavelength of the transmitted signal. Shadowing, interference, other background noise, and internal hardware loss are compensated with the link margin M_{l}.

B. Circuit Power Model

At any time instance, the transmitter works in one of the following three modes: the active mode in which signals are transmitted, the sleep mode in which no signal is transmitted, and the transient mode during which the switching between the active mode and the sleep mode happens. In this work we consider only the circuitry power of the active mode, and neglect the power consumption during the transient and sleep phase which is comparatively small. The circuit power model adopted here is based on the formulation in [4], where the total power consumption p of the transmitter in active mode consists of 3 parts as given by $p = p_{\mathrm{tx}} + p_{\mathrm{amp}} + p_{\mathrm{ct}} = (1+\alpha)p_{\mathrm{tx}} + p_{\mathrm{ct}}$. Besides the transmit power p_{tx}, an important part of the total power consumption comes from the power amplifier given as $p_{\mathrm{amp}} = \alpha \cdot p_{\mathrm{tx}}$, where $\alpha = \frac{\xi}{\eta} - 1$ with η the drain efficiency of the amplifier and $\xi = 3 \cdot \frac{\sqrt{M}-1}{\sqrt{M}+1}$ the peak-to-average ratio which depends on the MQAM constellation size. The power consumptions of the DAC, the transmit filters, the mixer, and the frequency synthesizer are included as a whole in p_{ct} and they constitute the constant part in p.

C. Data Transmission Model

Now we investigate the relation between the receive SNR and the instantaneous data rate, which could further lead us to the link between the energy consumption at the transmitter and the achievable throughput. The transmission mode employed by the energy harvesting node is referred to as the *mode of operation* (MOP), and it includes different parameters for uncoded and coded transmissions.

1) Uncoded MQAM: An upper bound on the uncoded bit error probability for MQAM is given by [4]

$$\pi_{\mathrm{b}} \leq \frac{4}{\log_2 M}\left(1 - \frac{1}{\sqrt{M}}\right) \mathrm{e}^{-\frac{3}{M-1}\cdot\frac{\gamma}{2}},$$

from which the minimum receive SNR to achieve a target BER $\pi_{\mathrm{b}}^{(\mathrm{rq})}$ can be computed. When the target BER is predefined and fixed, the required transmit power depends completely on the distance d and the constellation size M. Therefore, the MOP in the uncoded case corresponds to the single parameter M. We define the data rate in bit/sec as $r = \frac{\log_2 M}{T_{\mathrm{s}}}$.

2) Coded MQAM: In the coded scenario where forward error-correction codes are employed to control errors, we apply the *noisy channel coding theorem* [11] to obtain an upper bound on the codeword error probability. Let the modulation alphabet and coding rate be denoted with $\mathcal{A} = \{a_1, \ldots, a_M\}$ and R respectively. The *cutoff rate* of the channel with SNR γ and MQAM can be expressed as

$$R_0(\gamma, M) = \log_2 M - \log_2\left[1 + \frac{2}{M}\sum_{m=1}^{M-1}\sum_{l=m+1}^{M} e^{-\frac{1}{4}|a_l - a_m|^2\gamma}\right].$$

The noisy channel coding theorem states that there always exists a block code with block length l and binary code rate $R\log_2 M \leq R_0(\gamma, M)$ in bits per channel use, such that with maximum likelihood decoding the error probability $\tilde{\pi}$ of a codeword satisfies $\tilde{\pi} \leq 2^{-l(R_0(\gamma,M) - R\log_2 M)}$.

In order to apply this upper bound to the extensively used turbo decoded convolutional code, quantitative investigations have been done in [12] and an expression for the *equivalent block length* is derived based on link level simulations as $n_{\mathrm{eq}} = \beta_{\mathrm{c}} \ln L$, where the parameter β_{c} is used to adapt this model to the specifics of the employed turbo code, and L is the coded packet length. Consequently, the transmission of L bits is equivalent to the sequential transmission of L/n_{eq} blocks of length n_{eq} and has an error probability of

$$\pi = 1 - (1-\tilde{\pi})^{\frac{L}{n_{\mathrm{eq}}}} \leq 1 - \left(1 - 2^{-n_{\mathrm{eq}}(R_0(\gamma,M) - R\log_2 M)}\right)^{\frac{L}{n_{\mathrm{eq}}}}.$$

At the transmitter side, the processing power of the channel encoder is usually small enough to be neglected, hence the same power consumption model is applied to both the uncoded and coded transmissions. We assume that each data packet contains L_{o} bits of control overhead which are encoded together with the information bits. To this end, the transmission of a packet of L bits, which has been coded with code rate R, modulated with MQAM and has an error probability π, results in a data rate given by

$$r = \frac{(1-\pi)\log_2 M}{T_{\mathrm{s}}}\left(R - \frac{L_{\mathrm{o}}}{L}\right).$$

It can be observed that the data rate is dependent on the code rate, the constellation size, the transmit power, and also the length of the packet. All these parameters are included in one MOP for coded transmissions. For numerical simulations we have chosen 8 candidate Modulation and Coding Schemes (MCS) which are listed in Table II.

D. Energy Harvesting and Expenditure

An energy harvesting node gathers energy from the environment and stores them in its storage medium. Although the arrival of energy is often a random process and is not fully predictable, we assume here that the energy arrival in time slot $[\,0, T\,]$ is completely known in advance at the transmitter, so as to evaluate the performance limit of the system.

We utilize the *cumulative* model to describe the energy arrival as well as the energy expenditure of the transmitter. Let the nondecreasing functions $A(t)$ and $W(t)$ represent the

ISBN 978-3-8007-3482-5

Table I
SYSTEM PARAMETERS

$f_c = 2.5$ GHz	$B = 10$ kHz	$\frac{N_0}{2} = -174$ dBm/Hz
$\kappa = 3.5$	$\eta = 0.35$	$T_s \approx 1/B = 0.1$ ms
$P_{ct} = 98.2$ mW	$M_l = 30$ dB	$G_1 = 40$ dB
$\pi_b^{(rq)} = 10^{-3}$	$\beta_c = 32$	$L_o = 32$ bits

Table II
MODULATION AND CODING SCHEMES (MCS)

Index	Modulation Type	Code Rate R	$R \log_2 M$
1	BPSK	1/2	0.5
2	4-QAM	1/2	1
3	4-QAM	3/4	1.5
4	16-QAM	1/2	2
5	16-QAM	3/4	3
6	64-QAM	2/3	4
7	64-QAM	3/4	4.5
8	64-QAM	5/6	5

Table III
SIMULATION PARAMETERS

Parameter set index	$E_{\max}$ in Joule	Maximal energy per arrival
P.I	40	$0.6 \times E_{\max}$
P.II	100	$0.6 \times E_{\max}$
P.III	40	$0.4 \times E_{\max}$
P.IV	100	$0.4 \times E_{\max}$

total amount of energy that is available by time t and the total energy consumption of the node by time t, respectively. Due to causality, $W(t) \leq A(t)$ must be satisfied, $\forall t \in [0, T]$. Moreover, physical limitations on the energy storage that the node is equipped with give rise to a function $D(t)$ which represents the minimal amount of energy that has to be consumed by time t in order to avoid energy loss caused by storage overflow. Let $E_{\max}$ be the maximum amount of energy that the node can store. Assuming $E_{\max}$ is constant, we have $D(t) = \max(0, A(t) - E_{\max})$, $\forall t \in [0, T]$. No continuity requirement is imposed on $A(t)$ or $D(t)$, which means that our algorithms can be applied to both continuous and discrete energy arrival situations. Yet at a point of discontinuity on $A(t)$, let us denote it with t_0, we assume that $A(t_0^+) - A(t_0^-) < E_{\max}$, *i.e.*, there is no energy overflow caused by a very large instantaneous energy input. This guarantees $D(t) < A(t)$, $\forall t \in (0, T)$.

In order to maximize the throughput over $[0, T]$, all available energy should be used for data transmission and energy overflow should be avoided as much as possible, given that the data rate is an increasing function of the power consumption. With the continuous power model and no transmit power constraint, energy overflows can be avoided altogether. This means, $W(t) \geq D(t)$ has to be satisfied for $W(t)$ to be optimal. Since the energy consumption function $W(t)$ is bounded by $A(t)$ from above and by $D(t)$ from beneath, we refer to the functions $A(t)$ and $D(t)$ as the *boundary curves*. However, as the transmitter is now limited by the highest modulation order or the highest MCS available, it becomes incapable of storing and using all the energy it would be able to harvest. In such an occasion, part of the function $A(t)$ has to be decreased according to the time instance that the overflow happens as well as amount of energy that has been missed, which in turn causes decrement in $D(t)$. As a result of this adjustment, $W(t)$ is still bounded in between $A(t)$ and $D(t)$.

E. Throughput Maximization

The energy harvesting transmitter aims at maximizing the total throughput achieved from time 0 to T by properly adapting its MOP. The adaptation is based on the knowledge of the energy arrival process and the energy storage capacity of the node, and it should not violate the causality constraint. Such a design goal can be mathematically expressed by

$$\begin{aligned} \max \quad & I = \int_0^T r(t)\mathrm{d}t \\ \text{s.t.} \quad & W(t) = \int_0^t p(\tau)\mathrm{d}\tau \leq A(t), \\ & W(0) = 0, \end{aligned} \tag{1}$$

where the optimization is on the MOP as a function of time defined over $[0, T]$, and the dependencies of r and p on the MOP have been given previously. The condition $W(t) \geq D(t)$ is only necessary for optimality and is therefore not explicitly included in (1). We refer to the optimal MOP function for (1) as the *optimal transmission strategy* and denote the corresponding state function with W^*, which is also called the *optimal energy expenditure trajectory*. Notice that we drop the time index t in functions from now on.

III. OPTIMAL TRANSMISSION STRATEGY AND EFFICIENT MODES OF OPERATIONS

In our previous works [8][9] we have studied the throughput maximization problem at an energy harvesting transmitter with generic circuit power and data rate functions. To be more specific, we used the power consumption model $p = g(p_{tx})$ in the active mode where the function g is restricted to be convex or linear, and the data rate model $r = f(p_{tx})$ where the function f is strictly concave. Besides, f and g are both assumed to be nonnegative and monotonically increasing. Under these circumstances, a construction algorithm for finding W^* was designed and verified based on the method proposed in [13]. In the following we first review the key idea of the construction algorithm, and then discuss how the solution structure could be applied to the MOP optimization we are dealing with now.

A. Critical Slope based Construction Algorithm

When the power consumption function g is continuous on $[0, +\infty)$, the existence and uniqueness of W^* can be shown and the *optimality criterion* that *along the optimal trajectory W^* there do not exist any two points between which the part of W^* can be replaced with a straight line segment* is established [9]. Consider a time instance $t_0 \in [0, T)$ and let (t_0, α_0) satisfy $D(t_0) \leq \alpha_0 \leq A(t_0)$. Straight lines of nonnegative slopes starting from this point, denoted by $L_{(t_0,\alpha_0)}$, can be distinguished by whether they intersect with A or D first. Let $\mathcal{S}_A(t_0, \alpha_0)$ and $\mathcal{S}_D(t_0, \alpha_0)$ denote the sets of slopes which lead $L_{(t_0,\alpha_0)}$ to intersect with A and D first, respectively. Since $A > D$, $\forall t \in (0, T)$, the relation

ISBN 978-3-8007-3482-5

$\inf \mathcal{S}_A(t_0, \alpha_0) = \sup \mathcal{S}_D(t_0, \alpha_0)$ holds and we define this value as the *critical slope* at the respective point and denote it with $\beta(t_0, \alpha_0)$. The construction of W^* then proceeds in a simple recursive fashion: starting from $(0, 0)$, W^* takes the straight line segment with the critical slope at its current end point until it intersects with the boundary curve A or D. The next iteration begins then with the intersection point. Theorem was established in [13] proving the optimality of the constructed trajectory. We refer to the construction algorithm described above as the *basic algorithm*.

The positive constant part of circuit power may cause the function g to be discontinuous at $p_{\mathrm{tx}} = 0$, for the circuit power in sleep mode is assumed trivial. This leads to a positive *energy-efficient transmit power* p_{tx_0} below which the transmitter should not operate in active mode in order to maximize the throughput. To this end, the basic algorithm needs to be modified that in each iteration of the construction, the critical slope β at the current end point of W^* is compared with $p_0 = g(p_{\mathrm{tx}_0})$ to determine whether a sleeping period should take place. If $\beta > p_0$, W^* follows the straight line segment with slope β; otherwise, the transmitter is turned into sleep mode until it has to be activated, *i.e.*, to be able to employ the constant transmit power p_{tx_0} to reach the next intersection point, or to avoid energy overflow. Accordingly, this algorithm is named as the *modified algorithm*. The optimal trajectory in this scenario is not unique, but all optimums are *equivalent* in the sense that they lead to the same maximal throughput, and they differ only in the manner of time-sharing between the sleep mode and active mode in which p_{tx_0} is employed.

Since there is a one-to-one mapping between transmit power and the total power consumption, we can also view the achieved rate r as a function of the total power consumption p, namely $r = h(p)$. With optimal control theory *e.g.* [14], we find that the concavity of h plays the key role in the existence of W^* and whether our construction algorithm is still applicable. In fact, f being strictly concave and g being convex over $[0, +\infty)$ guarantees that h is strictly concave on $[0, +\infty)$, and the basic algorithm gives us the unique optimal W^* in this case. When g is discontinuous at $p_{\mathrm{tx}} = 0$, h is not a concave function but via the time-sharing of power $p = 0$ and $p = p_0$, the power-rate curve has been convexified so that the modified algorithm would give us one of the optimal W^*.

B. Energy-Efficient Modes of Operations

With the insights provided by studies on the continuous power case, we now aim at obtaining a concave dependency between r and p based on the discrete power-rate pairs representing all candidate MOPs. A given MOP is called *energy-efficient* if there is no other MOP that produces higher data rate but consumes less power. The Pareto boundary of the system is obtained by connecting the (p, r) points of all energy-efficient MOPs with straight lines, meaning that the points on these line segments are achieved via time-sharing of the two adjacent MOPs. The resulting curve defines the data rate r as a concave function of the power consumption p, but not strictly concave due to the linear parts.

In the uncoded case, we consider 4 MQAM schemes with $M = 2, 4, 16, 64$ which lead to 5 possible MOPs including the sleep mode. From Figure 1 we see that which MOP is energy-efficient depends on the distance d between the transmitter and the receiver. Lower modulation orders are in general inefficient with small d as p_{ct} is the dominant part in p, rendering the sleep mode a more attractive operation option. For d as large as 100 meters approximately, all modulation orders under consideration are energy-efficient.

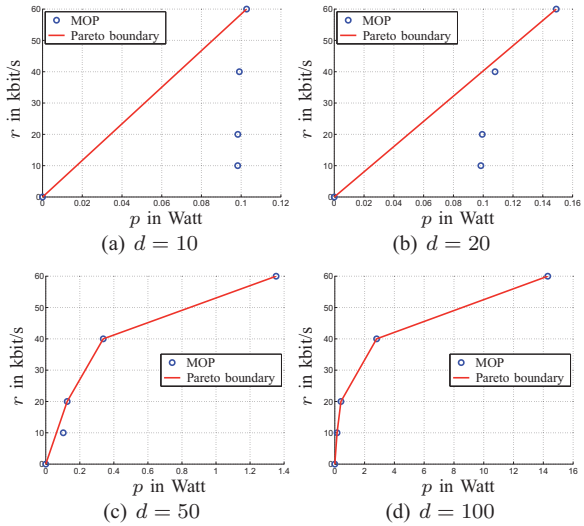

Figure 1. Pareto boundaries of power-rate pairs for uncoded transmission

The coded case is more complicated in that the packet length and packet error probability (PEP) also come into play. Given the number of symbols N_{s} in the coded packet, different MOPs can be obtained by varying the PEP. Energy-efficient MOPs are typically found with PEPs between 0.01 and 0.001. The Pareto boundary in this case is no longer the concatenation of several line segments between isolated energy-efficient MOPs, but rather contains several bending parts with continuous MOPs resulting from the continuously changing PEPs, as shown in Figure 2. Each bending part corresponds to the usage of one candidate MCS, and adjacent bending parts are connected with straight lines. We refer to the boundary points of bending parts as the *corner points*, which are involved in producing the required power consumption between two bending parts via time-sharing. Due to the fixed-length control overhead in each packet, Pareto boundaries of shorter packets lie below those of longer packets. With packet lengths much larger than L_{o}, the Pareto boundaries almost coincide, as can be seen in Figure 2(b). The power consumptions at the corresponding corner points decrease slightly with increasing N_{s}, but the decrement is small enough to be neglected. This means, we can assume that the energy-efficient MOPs obtained with different N_{s} have the same power consumption values but differ only in the achieved data rates. To this end, it suffices to find the power consumption values of energy-efficient MOPs for one relatively large N_{s}, record and use them for determining the involved MCS and for generating any required power

ISBN 978-3-8007-3482-5

consumption by time-sharing, no matter how long the packet actually is. The construction algorithm discussed in the next section is based on this assumption.

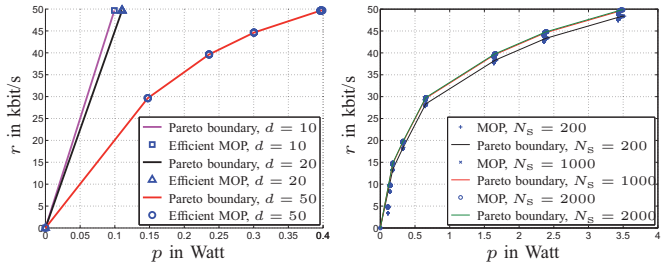

(a) $d = 10, 20, 50$ (b) $d = 100$

Figure 2. Pareto boundaries of power-rate pairs for coded transmission

IV. Construction of Optimal and Near-Optimal Energy Expenditure Trajectories

As mentioned earlier, given the boundary curves A and D, we can construct a trajectory with the basic algorithm which contains segments of the critical slopes. Such a trajectory is denoted with W_{b}, and it is optimal if transmit power can be adapted continuously, and the rate and circuit power functions satisfy certain conditions. We give an example of the curves A, D, W_{b} and other trajectories we construct in this section in Figure 3, where in Figure 3(a) the basic trajectory W_{b} with the designed boundary curves A and D is illustrated.

In the uncoded case, the Pareto boundary we have obtained indicates how each critical slope, which corresponds to the optimal power consumption at the time, should be achieved with the energy-efficient MOPs. To be more specific, for each segment of W_{b} with critical slope β, we find the power consumptions p_1 and p_2 of the adjacent energy-efficient MOPs on the Pareto boundary, and replace the part of W_{b} with line segments of slopes p_1 and p_2. The trajectory resulting from the replacement should not violate the boundary curves A and D. When the time period between two energy arrivals is much longer than the symbol duration, such a replacement is always possible. In fact, there are infinitely many valid replacements, each leading to an optimal trajectory W^*. One example is shown in Figure 3(b).

A similar idea is applied to the coded case: critical slopes between two corner points on the Pareto boundary are achieved with time-sharing, while critical slopes that fall within a bending part can be directly achieved with one MOP. In the former case a reconstruction of the segment of W_{b} is required, where the number of symbols used by each MOP needs to be determined. Unlike with uncoded transmission, the specific time-sharing manner will have an effect on the achieved data rate now. Generally speaking, the number of switches between the two involved MOPs should be made as small as possible. To this end, in our algorithm we employ each MOP as long as possible, until the boundary curve A or D requires a mode change. Although such a strategy is not always optimal, it is simple enough and gives good performance, while the optimal

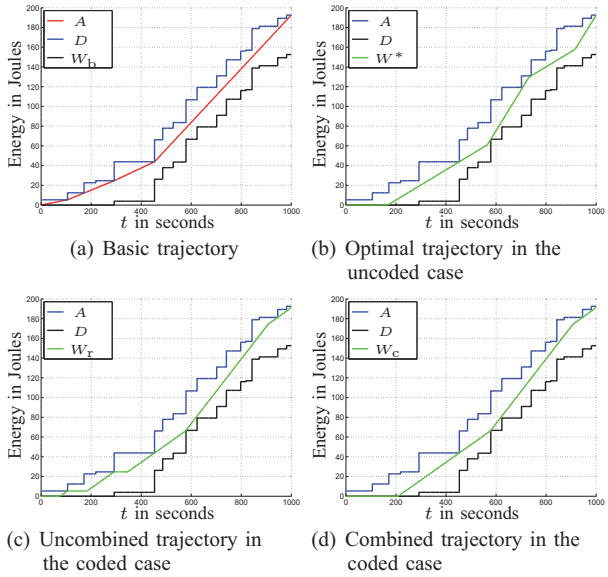

(a) Basic trajectory (b) Optimal trajectory in the uncoded case

(c) Uncombined trajectory in the coded case (d) Combined trajectory in the coded case

Figure 3. Exemplary energy boundary curves and constructed trajectories

time shares are very hard to compute. However, there are two special situations to be cared about. First, the rate/power ratio, *i.e.*, the bit per Joule value of the lower MOP, must be higher than that of the higher MOP in order to be energy efficient. When the power-rate point of the lower MOP lies below the line connecting the origin and the point representing the higher MOP, which could happen because of the control overhead in each packet, we see that using the lower MOP is not as good as turning the transmitter into sleep mode. Second, when the higher MOP produces a lower data rate than the lower MOP, we could consider not using the higher MOP for the current time share but employing the lower MOP the whole time. This could improve the throughput and spare some energy as well, which could be used in a following segment. The trajectory constructed as described above is denoted with W_{r} and shown in Figure 3(c).

An intuitive scheme to improve the throughput is to combine consecutive intervals with completely common MCS and treat them as one longer interval. Moreover, if consecutive intervals share one MCS and it is employed at the boundary between the intervals, a combination of packets could be done across the intervals. The trajectory we obtain after these combination operations is called the *combined trajectory* and denoted with W_{c}. Accordingly, W_{r} is termed as the *uncombined trajectory*. From Figure 3(d) we can observe that W_{c} is smoother than W_{r} and incurs less number of packets.

V. Simulation Results

For simulations we take the interval length $T = 1000$ seconds. The energy arrivals are at least 20 seconds away from each other, and after 20 seconds some more inter-arrival time following the negative exponential distribution with a mean of 40 seconds is expected. The amount of energy in each arrival is uniformly distributed from 0 to a certain percentage of the energy storage capacity $E_{\max}$. The parameters we vary

ISBN 978-3-8007-3482-5

in the simulations are summarized in Table III, and for each parameter set, 1000 realizations of the energy arrival during $[0, T]$ are generated and applied to our construction algorithm.

We first compare the throughput achieved with the transmission strategy given by the uncombined trajectory, denoted with $I(W_{\mathrm{r}})$, to the throughput achieved with the combined trajectory, denoted as $I(W_{\mathrm{c}})$, the results of which are depicted in Figure 4. As can be expected, larger throughputs are achieved with larger energy storage capacity and increased amount of energy arrivals. The performance gap is smaller at short distances due to the limitation in the highest MCS that is available, *i.e.*, the available energy might not be fully utilized in those cases. The improvement offered by the combined trajectory is rather trivial, not exceeding 1% on average according to Figure 4(b). As combining adjacent packets with identical MCS is not a complex task, it might still be worth doing in some scenario, especially when the control overhead in each packet is relatively long.

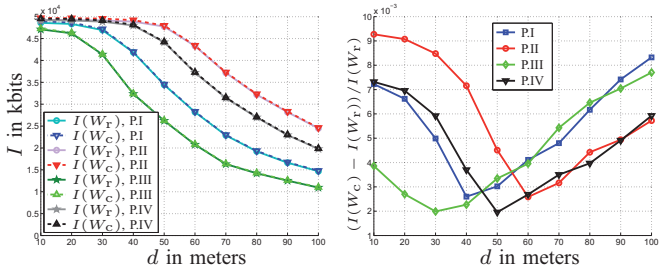

(a) Average throughput (b) Improvement in throughput by using the combined algorithm

Figure 4. Average throughput and algorithm comparisons

The average throughput achieved with uncoded and coded transmissions are shown in Figure 5, with varied parameters and as dependent on the distance d. For the coded case the throughput of the combined trajectory is shown. It can be observed that with the transmitter and receiver less than 30-40 meters apart, the performance of coded transmission is close to or worse than that of uncoded transmission, which is also suggested by Figure 1 and Figure 2. That means, at such short distances, it is not worthwhile to transmit the redundancy in order to reduce packet error probability. Coded transmission becomes clearly favourable when the the transmitter and receiver are further apart, *e.g.*, for $d \geq 50$ meters.

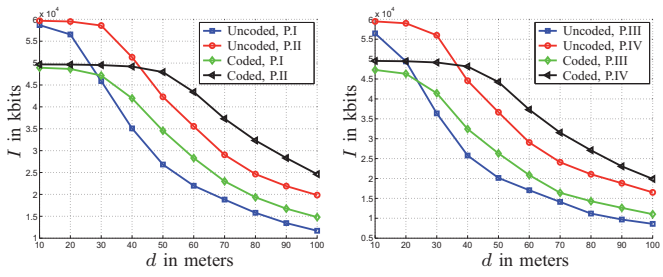

(a) Parameter sets I and II (b) Parameter sets III and IV

Figure 5. Average achieved throughput in uncoded and coded scenarios

VI. Conclusion

The throughput maximization problem of an energy harvesting transmitter is investigated in this work. We focus on the scenario that the transmitter sends data over a single invariant link, and it has a priori information about the energy arrivals during the time slot of interest. Not only transmit power, but also circuit power of various components in the RF circuitry are considered in the total power consumption model of the transmitting node. For each candidate mode of operation, the total power required to employ it and the data rate it offers can be computed. To this end, we characterise both uncoded and coded transmissions of data by the respective Pareto boundaries, which are determined by the energy-efficient MOPs on the power-rate graph. Consequently, the critical slope based construction algorithm of the optimal energy expenditure trajectory can be adapted to the discrete-MOP case with the modification, that the critical slopes are now achieved with proper time-sharing of energy-efficient MOPs as indicated by the Pareto boundary. All algorithms proposed in the work are verified and illustrated with numerical simulations, based on which we also compare the utilization of uncoded and coded transmissions with respect to the distance between the transmitter and receiver.

References

[1] D. Niyato, E. Hossain, M. M. Rashid, V. K. Bhargava, *Wireless Sensor Networks with Energy Harvesting Technologies: A Game-Theoretic Approach to Optimal Energy Management*, IEEE Wireless Communications, August 2007, vol. 14, pp. 90-96.

[2] M. Gorlatova, A. Wallwater, G. Zussman, *Networking Low-Power Energy Harvesting Devices: Measurements and Algorithms*, IEEE INFOCOM 2011, April 2011.

[3] S. Sudevalayam, P. Kulkarni, *Energy Harvesting Sensor Nodes: Survey and Implications*, IEEE Communications Surveys & Tutorials, vol. 13, no. 3, 2011.

[4] S. Cui, A. J. Goldsmith, *Energy-constrained modulation optimization*, IEEE Transactions on Wireless Communications, Sept. 2005, vol. 4, issue 5, pp. 2349-2360.

[5] Q. Chen, M. C. Gursoy, *Energy-Efficient Modulation Design for Reliable Communication in Wireless Networks*, 43rd Annual Conference on Information Sciences and Systems (CISS 2009), March 2009.

[6] K. Tutuncuoglu, A. Yener, *Short-Term Throughput Maximization for Battery Limited Energy Harvesting Nodes*, IEEE International Conference on Communications 2011, Kyoto, Japan, June 2011.

[7] K. Tutuncuoglu, A. Yener, *Optimum Transmission Policies for Battery Limited Energy Harvesting Nodes*, IEEE Transactions on Wireless Communications, vol. 11, no. 3, March 2012.

[8] Q. Bai, J. Li, J. A. Nossek, *Throughput Maximizing Transmission Strategy of Energy Harvesting Nodes*, Third International Workshop on Cross-Layer Design (IWCLD 2011), November 2011.

[9] Q. Bai and J. A. Nossek, *Throughput Maximization for Energy Harvesting Nodes with Generalized Circuit Power Modelling*, the 13th IEEE International Workshop on Signal Processing Advances in Wireless Communications (SPAWC 2012), June 2012.

[10] A. Goldsmith, *Wireless Communications*, Cambridge University Press 2005.

[11] R. G. Gallager, *Information Theory and Reliable Communication*, John Wiley and Son, 1968.

[12] B. Zerlin, M. T. Ivrlač, W. Utschick, J. A. Nossek, I. Viering and A. Klein, *Joint optimization of radio parameters in HSDPA*, in IEEE 61st Vehicular Technology Conference VTC 2005-Spring, vol. 1, pp. 295-299.

[13] M. Zafer, E. Modiano, *A Calculus Approach to Energy Efficient Data Transmission with Quality-of-Service Constraints*, IEEE/ACM Transactions on Networking, vol. 17, pp. 898-911, March 2010.

[14] E. R. Pinch, *Optimal Control and the Calculus of Variations*, Oxford University Press, 1993.

ISBN 978-3-8007-3482-5